Key Engineering Materials
ISSN: 1662-9795, Vol. 926, pp 683-689
doi:10.4028/p-3rk19y

Submitted: 2021-12-01
Revised: 2022-02-01
Accepted: 2022-02-08
Online: 2022-07-22

Manufacture of Defined Residual Stress Distributions in the Friction-Spinning Process: Driven Tool and Subsequent Flow-Forming

Frederik Dahms[*,1,a], Werner Homberg[1,b]

[1]Paderborn University, Forming and Machining Technology, 33098 Paderborn, Germany

[a]fd@luf.upb.de, [b]wh@luf.upb.de

Keywords: Friction-Spinning, Residual Stress, Incremental Forming, Aluminium Forming.

Abstract. Friction-spinning as an innovative incremental forming process enables large degrees of deformation in the field of tube and sheet metal forming due to a self-induced heat generation in the forming zone. This paper presents a new tool and process design with a driven tool for the targeted adjustment of residual stress distributions in the friction-spinning process. Locally adapted residual stress depth distributions are intended to improve the functionality of the friction-spinning workpieces, e.g. by delaying failure or triggering it in a defined way. The new process designs with the driven tool and a subsequent flow-forming operation are investigated regarding the influence on the residual stress depth distributions compared to those of standard friction-spinning process. Residual stress depth distributions are measured with the incremental hole-drilling method. The workpieces (tubular part with a flange) are manufactured using heat-treatable 3.3206 (EN-AW 6060 T6) tubular profiles. It is shown that the residual stress depth distributions change significantly due to the new process designs, which offers new potentials for the targeted adjustment of residual stresses that serve to improve the workpiece properties.

Introduction

Friction-spinning as an innovative incremental hot-forming process enables large degrees of deformation in the field of tube and sheet metal forming due to a friction-induced heat generation in the forming zone in an efficient way [1]. The self-induced partial heating of the components not only enables a significantly higher forming rate, but also a defined influence on the mechanical properties and microstructure. For example, the forming of flanges by friction-spinning of tubes is dominated by shearing in the tangential direction and by bending-like forming in the radial direction and the force and temperature profiles are radius depending [2]. These complex thermomechanical conditions lead to non-uniform residual stress distributions which arise due to plastic deformation misfits between different regions which are classified as mechanical, thermal and chemical [3]. Stress relief heat treatment and plastic deformation can relieve residual stresses [4]. Residual stresses can lead to component failure [5], but in this context locally adapted residual stress distributions are intended to improve the quality and functionality of the friction-spinning workpieces [6] [7], e.g. by delaying or triggering failure in a defined way.

Regarding residual stress adjustments in aluminium-parts (e.g. flanges), preliminary investigations have shown that with the conventional process design, with a fixed tool, the rotation speed has the greatest effect on the gradient of the residual stress depth distribution [2]. Using the methods of design of experiments the effects and interactions of the process parameters were determined and empirical models were developed on this basis. For targeted residual stress adjustments, these models were implemented in a run-to-run predictive control. Furthermore, a 3D DIC residual stress measurement method was investigated and improved to enable more efficient residual stress adjustments [8]. However, since the effects were not sufficient to completely change the character of the residual stress distributions a new tool and process design have been developed. These include a driven-tool system and an optional subsequent flow-forming process, for the targeted adjustment of residual stresses in the friction-spinning process. Comparable incremental processes such as flow-forming [9] [10], metal-spinning [11] [12] or tube-spinning [13] offer the potential to introduce especially tensile

residual stress distributions into the component, while compressive and tensile residual stresses occur, for example, in flanges formed by friction-spinning of tubes [2].

This paper presents the investigations on the new process design regarding the influences of the tool rotation and the subsequent flow-forming on the residual stress depth distributions compared to those of the standard friction-spinning process. Therefore, residual stress depth distributions are measured with the standardized incremental hole-drilling method [14] [15], and residual stress surface distributions by x-ray diffraction [16]. The workpieces (tubular part with a flange) are manufactured using heat-treatable 3.3206 (EN-AW 6060) tubular profiles.

Experimental Setup

In the following the new tool and process designs are described and the experimental investigations of the new process characteristics and the resulting residual stress distributions are presented. Generally, the workpieces, tubular parts with a flange, are manufactured using heat-treatable 3.3206 (EN-AW 6060 initial temper state T6) tubular profiles with the LUF in-house design friction-spinning machine (FSV) which is computer controlled by Sinumerik 840D by Siemens AG, Germany. The main spindle drive has a power of 100 kW.

For the new process designs, a 25 kW tool-drive servo motor was integrated into the tool-axis to drive the tool by a v-belt and is controlled by the computer control of the Sinumerik 840D of the FSV. Another axis, which is also controlled by the Sinumerik, allows to be used for flow-forming. The flow-forming roller has a diameter of d_R = 200 mm, and angle of 15° and is made of the steel 1.2379 hardened and tempered to 62 HRC.

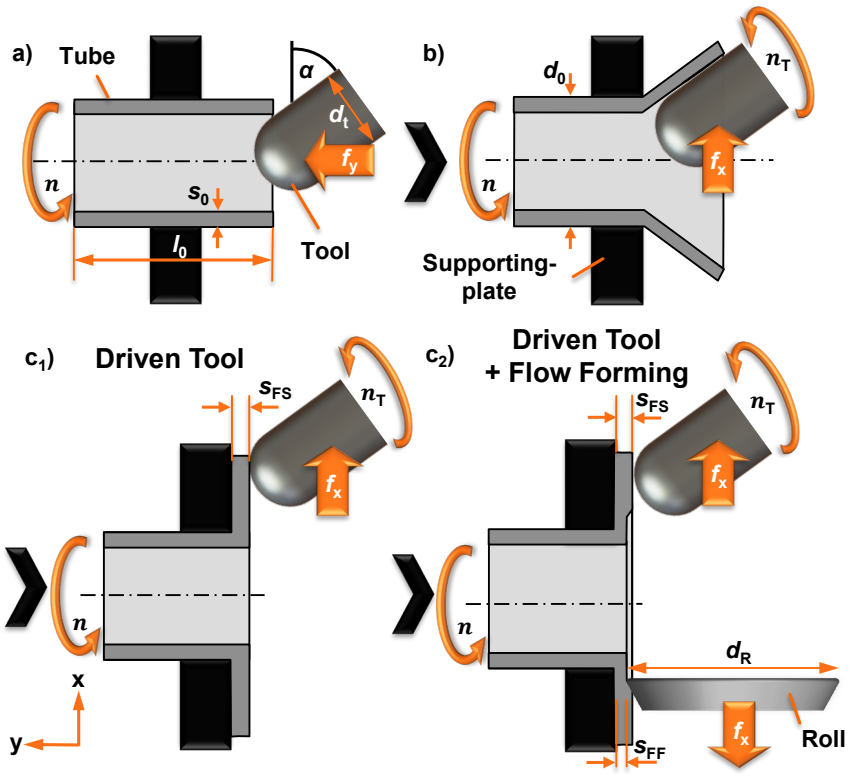

Figure 1. Friction-spinning process with driven tool and subsequent flow-forming.

The new innovative friction-spinning process-design with the new tool systems is subdivided into the pre-friction phase and the flange-forming phase. In the pre-friction phase, heat is induced to the workpiece by friction with the stationary forming tool (*cf.* **Figure 1**, a – b). In the subsequent flange-forming phase, the tool is fed radially (feed rate *f*) and driven with the tool rotation speed n_T either in synchronism or counter-rotation to the workpiece (*cf.* **Figure 1**, b – c_1). In this phase, additional forming can be carried out by a subsequent flow-forming process in the radial direction (*cf.* **Figure 1**, c_2). In order to determine the new process characteristics, temperature profiles and the electrical power of the tool-drive are measured.

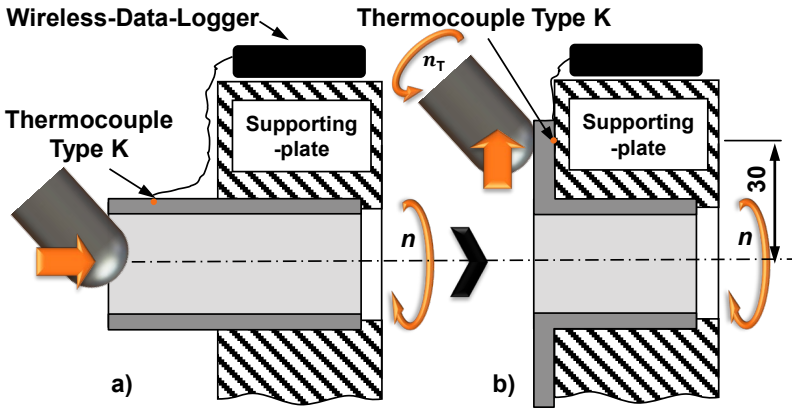

Figure 2. Wireless temperature-measuring set-up in the friction-spinning process.

The complexity of temperature measurements in the friction-spinning process results from its process characteristics (friction of the tool on the surface and rotation of the workpiece) and with aluminium especially optical temperature measurements are not feasible due to its complex emissivity characteristics [17]. In addition, a basic black coating on the driven tool does not endure the forming process, so that reflections of the ambient heat radiation cannot be ruled out.

Therefore, type k thermocouples were used with the radio data logger (measuring amplifier) Cobra SMARTsense, PHYWE Systems, Germany. The thermocouples type k are mechanically joined in corresponding holes at a discrete measuring point (here in R = 30 mm) (*cf.* **Figure 2)**. This means that the measuring amplifier can be mounted on the rotating supporting-plate and the measured values can be transmitted wirelessly, which will provide new important insights into the temperature profile of the friction-spinning process, also in the areas that cannot be measured optically. With the new approach, heating and cooling curves of this process can be used to build up models of the generation of thermal residual stresses in the friction-spinning process.

Finally, the initial findings of the residual stress evaluations of the new process designs are presented. For comparability, the process parameters of the standard process are applied to the new processes. Residual stress depth measurements are performed on the upper side of the flange in a distance of R = 30 mm from the centre-point. Hole drilling is operated by Vishay RS 200 and 1.6 mm inverted-cone endmills. Vishay Micro Measurements' strain-gauge rosettes CEA-13-062UM-120 are applied. Strains are processed with the universal measuring amplifier HBM MX 440 in three-wire half-bridge circuit with 120-ohm precision resistors. Residual stresses are calculated by H-Drill 4.0 according to ASTM E837-20 [15].

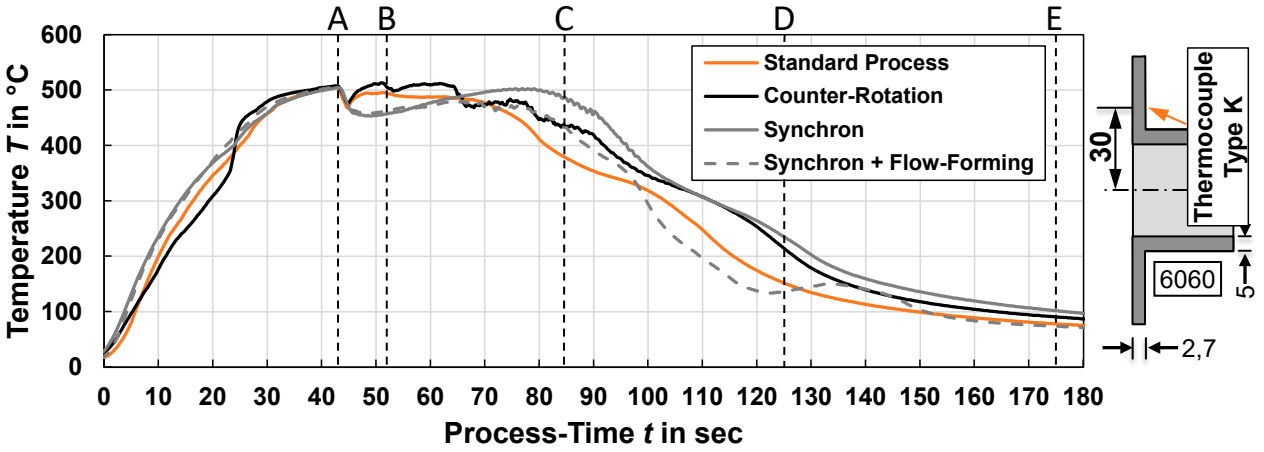

Figure 3. Temperature curves of the new process strategies in the friction-spinning process measured with thermocouple type k (Aluminium 6060). Rotation speed of the workpieces n = 900 rpm, rotation speed of the tool n_T = 800 rpm, feed-rate of the tool f = 0.5 mm/s, feed-rate of the roller (flow-forming) f_R = 0.5 mm/s.

Experimental Investigations

Process characteristics. First, the process characteristics are determined so that the subsequent analysis of the residual stress profile can be discussed in the context of the conventional friction-spinning process. **Figure 3** shows the temperature profiles of the three new process variants in comparison to the standard friction-spinning process. The friction-spinning process with driven tool leads to a maximum temperature of T_{max} = 510 °C with a wall thickness reduction from s_0 = 5 mm initial thickness to s = 2.7 mm flange thickness. The relative drive direction influences the maximum temperatures only slightly.

However, higher temperatures are maintained over a longer period of time by driving the tool. The temperatures decrease for a short time after the changeover point, from axial to radial feeding of the tool (*cf.* **Figure 3** (A)). This is due to the tool is separated from the workpiece for a time of less than one second in order to ensure a controlled start of the drive of the tool. After re-establishing contact between the workpiece and the tool, the maximum workpiece temperature is not reached again as quickly in the synchronous drive as in the standard process or the counter-driven process (B). After that, the temperatures decrease steadily. By driving the tool, the workpiece temperature is clearly higher at the end of the forming phase (C to D) as in the standard process. The engagement of the roller in this phase significantly reduces the workpiece temperature (C). By separating the tool from the workpiece, the friction-spinning process is completed (D). With the additional flow-forming process, there is an intermediate increase in the workpiece temperature at point D, whereby the temperature adapts to the curve of the other process variants until the end of the flow-forming operations (E).

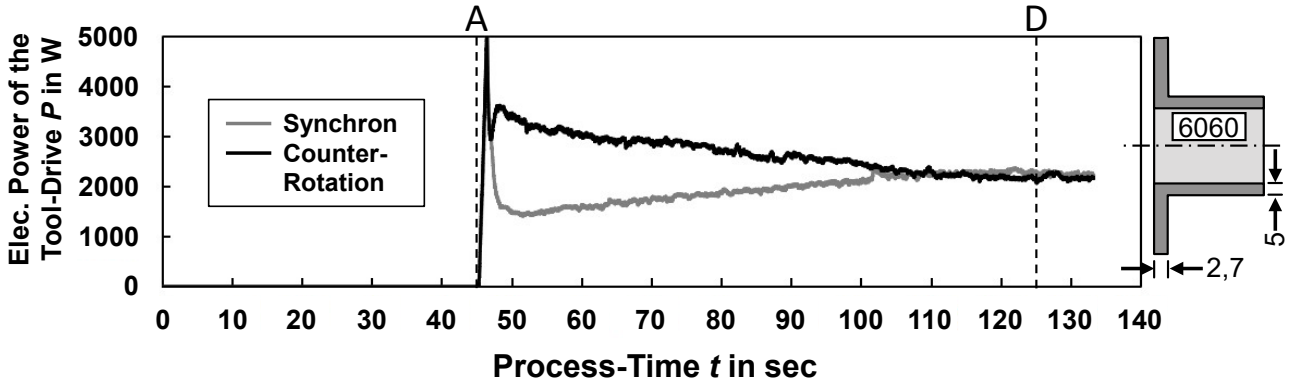

Figure 4. Power supply to the driven tool in the friction-spinning process (Aluminium 6060). Rotation speed of the workpieces n = 900 rpm, rotation speed of the tool n_T = 800 rpm, feed-rate of the tool f = 0.5 mm/s.

The active electrical power consumption of the tool-drive to drive the tool in counter-rotation or synchron to the workpiece, which is measured by the drive-system, is shown in **Figure 4**. When starting the tool-drive (A), there is a short, strong power increase, which immediately drops again. In the following, the tool-drive needs in maximum 3500 W to maintain the tool rotation speed of n_T = 800 rpm in counter-rotation to the workpiece rotation (n = 900 rpm). To maintain the tool rotation speed of n_T = 800 rpm synchron driven to the workpiece it needs at least 1500 W. The power for the counter-rotation of the tool decreases till the end of the friction-spinning process (D), whereas the power for the synchron-rotation of the tool increases till the end of the friction-spinning process with 2200 W (D).

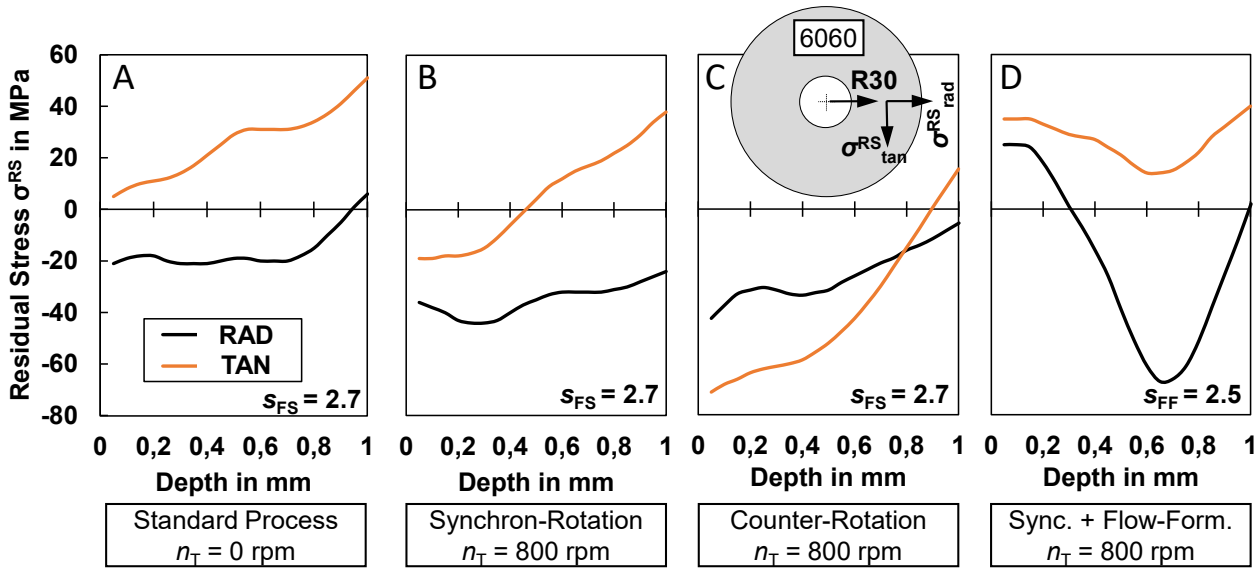

Figure 5. Residual stress depth distribution measured with the HDM from the upper side of the flange (Aluminium 6060). Rotation speed of the workpieces n = 900 rpm, feed-rate of the tool f = 1.5 mm/s, feed-rate of the roller (flow-forming) f_R = 1.5 mm/s. Flange thickness after friction-spinning s_{FS} = 2.7 mm and after flow-forming s_{FF} = 2.5 mm.

Residual stress depth distributions. In **Figure 5** the residual stress depth distributions of the new friction-spinning process-designs with the driven tool are compared to the standard process [2] with a fixed tool. Residual stresses are measured on the upper-side of the flange at R = 30 mm using the incremental hole-drilling method.

For the standard friction-spinning process it is characteristic that compressive residual stresses occur in the radial direction and tensile residual stresses in the tangential direction [2]. With a rotation speed of n = 900 rpm and a feed-rate of f = 1.5 mm, in the radial direction the compressive residual stresses tend to be constant in the surface with max. of σ^{RS}_{rad} = -20 MPa with a slightly decreasing tendency to the core (*cf.* **Figure 5**, A). In the tangential direction, there are strongly graded tensile residual stresses that increase with depth (max. σ^{RS}_{tan} = 50 MPa).

When additionally driving the tool with n_T = 800 rpm in synchron rotation to the workpiece, the radial compressive residual stresses increase to max. σ^{RS}_{rad} = -45 MPa (*cf.* **Figure 5**, B). The tangential residual stresses are compressive near the surface (σ^{RS}_{tan} = -20 MPa) and tensile in the core (σ^{RS}_{tan} = 40 MPa). Driving the tool in counter-rotation with n_T = 800 rpm, only slightly influences the radial compressive residual stresses, but the tangential residual stresses in the surface increase to a max. of σ^{RS}_{tan} = -70 MPa and decrease to the core up to approx. σ^{RS}_{rad} = 15 MPa (*cf.* **Figure 5**, C). The subsequent flow-forming (*cf.* **Figure 5**, D) in combination with the synchron rotating tool (n_T = 800 rpm) leads to a whole new character of the residual stress depth distribution, compared to that of the standard process design (*cf.* **Figure 5**, A) [2]. In the surface there are tangential residual stresses in both directions (σ^{RS}_{rad} = 25 MPa and σ^{RS}_{tan} = 35 MPa). In the depth of 0.6 mm there are tensile residual stresses in tangential direction and a peak of compressive residual stresses in radial direction (σ^{RS}_{rad} = -70 MPa). In the core (depth of 1.0 mm) there are also tensile residual stresses in the tangential direction (σ^{RS}_{rad} = 25 MPa and σ^{RS}_{tan} = 40 MPa). Thereby, the stresses in radial direction are zero and tend to tensile residual stresses with increasing depth, following the gradient of the curve.

Discussion. In the experimental investigations, first the new process characteristics and the resulting residual stress distributions were evaluated. The temperature profile, in terms of maximum temperatures, is not significantly changed by the new process designs, but the temperatures are kept high for longer by driving the tool during the forming-phase and are dissipated more quickly by flow-forming during this phase.

The comparison of the active electrical power consumption of the tool-drive shows the power needed to work against or with the rotation of the workpiece. In this regard, it can be seen that the required torque, which is proportional to the power at constant rotation speed, decreases in the

progression of the process. This is because the contact area between the tool and the workpiece decreases and with it the torque required to rotate the tool. Inversely, the torque increases when the tool is driven less by friction with the workpiece. Finally, the tool drive needs more power when it is not engaged than in synchronous rotation with workpiece contact.

The corresponding residual stress depth evaluations show that driving the tool causes compressive residual stresses in tangential direction, so that compressive residual stresses are present in both directions near the surface and that subsequential flow-forming changes the character of the residual stresses significantly. In principle, it can be assumed that driving the tool influences the stress state respectively the material flow in the forming zone due to the new type of relative motion in the contact area. It is less plausible that the changes in the residual stress profile are due to the change in the temperature profile, as they only deviate slightly from the standard process. The great influence of the stress state is also evident in the subsequential flow-forming with its different stress state that significantly changes the residual stress profile. The residual stress profile resulting from the friction-spinning process with driven tool is superimposed by the flow-forming caused tensile residual stresses in the surface layer.

The novel residual stress depth distribution characteristics achieved by the new process designs provide new potential for the targeted adjustment of residual stresses depth profiles, which serve to improve workpiece properties. For example, it is possible to adjust compressive residual stresses in both directions of the flange surface layer by the new process designs, which supports the durability of the workpiece under dynamic loads.

Further investigations must be carried out on this, also on the corresponding process characteristics, in particular the new stress states. Thereby, using the methods of design of experiments, the aim is to create empirical models in order to integrate them into a run-to-run predictive control. The application of machine learning methods is also conceivable for this purpose. Additionally, the driven tool system will be redesigned with a new drive train to allow a wider range of process parameters to be investigated.

Summary

In this paper, new innovative friction-spinning process and tool designs were presented that can significantly change the character of residual stresses in flanges formed by friction-spinning of tubes (Aluminium 6060 T6) compared to those of the standard friction-spinning process. It is shown how the residual stress distribution can be significantly influenced by driving the tool and by additional subsequent flow-forming. The novel residual stress depth distribution characteristics achieved by the new process designs provide new potential for the targeted adjustment of residual stresses depth profiles, which serve to improve workpiece properties. Furthermore, essential process characteristics, such as the temperature profile, were investigated. These are initial findings that require further research. Therefore, with the aim of model building, further investigations using the methods of design of experiments are intended.

Acknowledgment

The authors would like to thank the German Research Foundation (DFG) for funding the research project “HO 2356/14-1”, with the project number 410908773: "Manufacture of defined residual stress in friction assisted spinning and flow forming". The research work conducted in this project is the basis of the paper.

References

[1] B. Lossen, A. Andreiev, M. Stolbchenko, W. Homberg, and M. Schaper, "Friction-Spinning - Grain Structure Modification and the Impact on Stress/Strain Behaviour," Journal of Materials Processing Technology, vol. 261, pp. 242–250, 2018, doi: 10.1016/j.jmatprotec.2018.06.015.

[2] F. Dahms and W. Homberg, "Manufacture of Defined Residual Stress Distributions in the Friction-Spinning Process: Investigations and Run-to-Run Predictive Control," metals, vol. 12, no. 1, p. 158, 2022, doi: 10.3390/met12010158.

[3] P. J. Withers and H. Bhadeshia, "Residual stress. Part 2 – Nature and origins," Materials Science and Technology, vol. 17, no. 4, pp. 366–375, 2001, doi: 10.1179/026708301101510087.

[4] J. S. Robinson, T. Pirling, C. E. Truman, and T. Panzner, "Residual stress relief in the aluminium alloy 7075," Materials Science and Technology, vol. 33, no. 15, pp. 1765–1775, 2017, doi: 10.1080/02670836.2017.1318243.

[5] P. J. Withers, "Residual stress and its role in failure," Rep. Prog. Phys., vol. 70, no. 12, pp. 2211–2264, 2007, doi: 10.1088/0034-4885/70/12/R04.

[6] M. Sticchi, D. Schnubel, N. Kashaev, and N. Huber, "Review of Residual Stress Modification Techniques for Extending the Fatigue Life of Metallic Aircraft Components," Appl. Mech. Rev., vol. 67, no. 1, p. 10801, 2014, doi: 10.1115/1.4028160.

[7] G. Maeder, "The use of residual stresses in automotive industry," Revue De Metallurgie-Cahiers D Informations Techniques, Vol.94 (2), p. 199, 1997.

[8] F. Dahms and W. Homberg, "Investigations and Improvements in 3D-DIC Optical Residual Stress Analysis—A New Temperature Compensation Method," in The Minerals, Metals & Materials Series, FORMING THE FUTURE: Proceedings of the 13th international conference on the Technology of Plasticity, G. Daehn, J. Cao, B. Kinsey, E. Tekkaya, A. Vivek, and Y. Yoshida, Eds.: Springer Cham., 2021, pp. 2249–2259.

[9] X. Song et al., "Diametrical growth in the forward flow forming process: simulation, validation, and prediction," Int J Adv Manuf Technol, vol. 71, 1-4, pp. 207–217, 2014, doi: 10.1007/s00170-013-5492-x.

[10] D. Tsivoulas, J. Da Quinta Fonseca, M. Tuffs, and M. Preuss, "Effects of flow forming parameters on the development of residual stresses in Cr–Mo–V steel tubes," Materials Science and Engineering: A, vol. 624, pp. 193–202, 2015, doi: 10.1016/j.msea.2014.11.068.

[11] Z. Li and X. Shu, "Residual stress analysis of multi-pass cold spinning process," Chinese Journal of Aeronautics, 2021, doi: 10.1016/j.cja.2021.07.004.

[12] O. Music, J. M. Allwood, and K. Kawai, "A review of the mechanics of metal spinning," Journal of Materials Processing Technology, vol. 210, no. 1, pp. 3–23, 2010, doi: 10.1016/j.jmatprotec.2009.08.021.

[13] C. H. Gür and E. B. Arda, "Effect of tube spinning and subsequent heat treatments on strength, microstructure and residual stress state of AISI/SAE type 4140 steel," Materials Science and Technology, vol. 19, no. 11, pp. 1590–1594, 2003, doi: 10.1179/026708303225008022.

[14] G. S. Schajer and P. S. Whitehead, "Hole-Drilling Method for Measuring Residual Stresses," Synthesis SEM Lectures on Experimental Mechanics, vol. 1, no. 1, pp. 1–186, 2018, doi: 10.2200/S00818ED1V01Y201712SEM001.

[15] Test Method for Determining Residual Stresses by the Hole-Drilling Strain-Gage Method, ASTM E837-20, West Conshohocken, PA. [Online]. Available: www.astm.org

[16] M. Fitzpatrick, A. Fry, P. Holdway, F. Kandil, J. Shackleton, and L. Suominen, "Determination of Residual Stresses by X-ray Diffraction: Issue 2," Measurement Good Practice Guide. National Physical Laboratory, 2005, 2005.

[17] C.-D. Wen and I. Mudawar, "Modeling the effects of surface roughness on the emissivity of aluminum alloys," International Journal of Heat and Mass Transfer, vol. 49, 23-24, pp. 4279–4289, 2006, doi: 10.1016/j.ijheatmasstransfer.2006.04.037.